Supporting Information

Photopolymerizing carbazole-based monomers in dilute media: prototyping organic wires with nanoscale thickness control.

Jennifer Calderon-Mora[a], Ali Dabbous[a], Baptiste Maillot[a], Rasta Ghasemi[a], Jean Frédéric Audibert[a], Fabien Miomandre[a]*, Vitor Brasiliense[a]*

S1) Absorption Spectra of Rhodamine and Rhodamine dyads

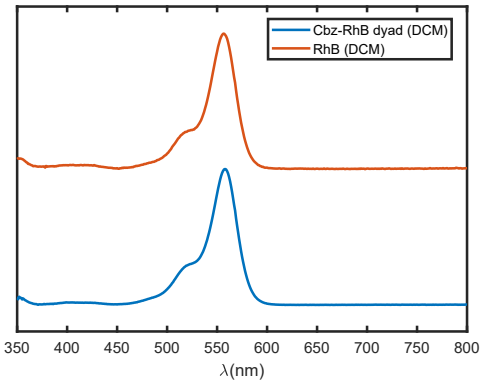

Figure S1.1 Comparison of the absorption spectra of Cbz-RhB dyads and RhB solutions.

S2) Infrared Vibrational analysis of photografted layers

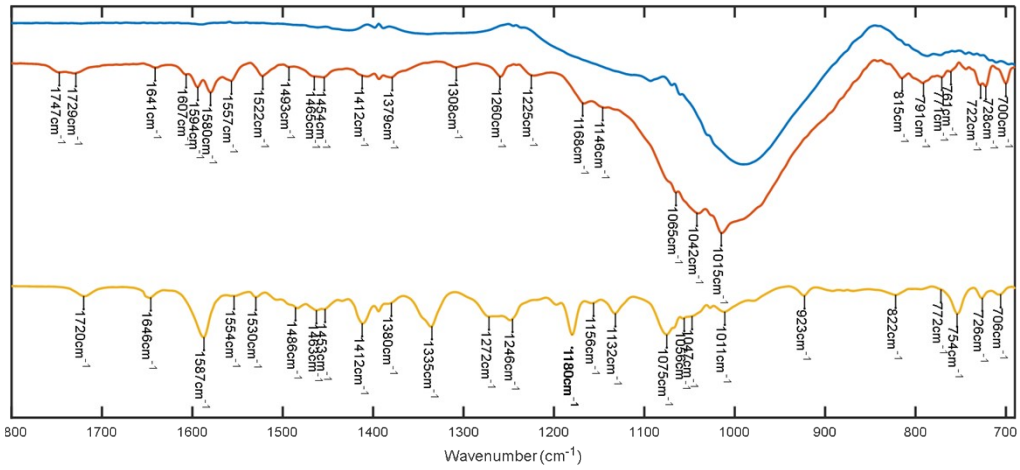

Figure S2.1 Infrared spectrum of the photopolymerized pCbz-RhB grid (orange), compared to the background IR of a ITO layer (blue). The data, also reported in Fig.3A, is showcased here at larger scale, enabling better identification of the observed vibrational band. Infrared spectra of the monomeric dyad powder is also shown, confirming the identity of the polymerized layer and facilitating band assignement (yellow)

The global IR spectrum, collected from grid samples as described in the main text and reported in Fig.3A, is reproduced here at larger scale, enabling a more careful examination of its characteristic bands. We also compare the resulting spectrum with a powder IR spectrum of dyad molecules, showing that analogue bands can be find for almost all vibrations. The positions of the main detected bands are indicated in the image, while the discussion that follows provides a tentative band

assignment based on characteristic group vibration frequencies and literature data. Unambiguous band assignment of several of the discussed modes is difficult without extra experiments, however comparison with reported characteristic vibrational modes of carbazole, rhodamines and related compounds is possible. Additionally, the IR spectra of photopolymerized layer and the dyad in the crystalline state can be readily compared, clearly demonstrating that both moieties remain intact on the final photopolymerized material.

Noteworthy, since there the quantity of material on the surface is small, the bands are not very intense, which, associated to the complexity of the material, casts difficulties onto the band assignment process. Yet, a tentative band assignment is still provided in the table below, based on the folowing discussion.

Carbonyl Stretching (ν) modes (Region 1700-1800 cm^{-1}). The region between 1700 and 1800 cm^{-1} contains very characteristic C=O stretching modes[1]. The presence of bands in this region is expected due to the ester function present in the RhB bands. As indicated in Fig.S6.2, two bands are indeed observed, at 1729 and 1747 cm^{-1} the region, suggesting two chemical environments are present.

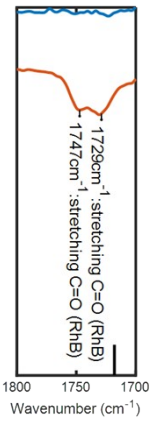

Figure S2.2 Focus on the 1700-1800 region. The bottom dark line indicates the position of the vibration on solid rhodamine samples [2]

C-O Stretching modes. Following the identification of C=O bands in the 1700-1800 cm^{-1} range, we also expect to observe C-O stretching modes from the ester moiety, which usually arise in the 1000-1300 cm^{-1} range[1]. Compared to their C=O stretching counterparts, their presence is however more delicate to assign, as several other frequencies are present in the same region. On the basis of frequent observation of saturated esters in the 1163-1210 cm^{-1} region [1], we tentatively assign the 1168cm^{-1} band to this vibration. It must be noted that ν(C-O) modes has alternatively been assigned to the 1225 cm^{-1} band due to the presence of 1242 cm^{-1} band[2]

In plane C-H bending (δ) modes (1000-1300cm^{-1}) Similarly to the C-H vibration on the 700-850 cm^{-1} region (see below), polymerization of carbazole moieties is expected to be accompanied by decrease of signals associated to bending δ_{IP} (C-H) modes associated to 1,2 disubstituted rings, usually observed in the 1040-1080 cm-1 and 1100-1150 cm^{-1} regions[6]. As shown in Fig.S2.1 we in the monomeric dyad we observe two weak modes at 1047-1056 cm^{-1}, a stronger mode at 1075 cm^{-1} and a band at 1132 cm^{-1}. After polymerization, the bands at 1047-1056 cm^{-1} can still be detected at 1042cm^{-1}, while the strong band at 1075 and 1132 are strongly depleted. Based on these observations, the 1047 cm^{-1} is assigned to δ_{IP}(C-H) on RhB external ring, while the 1075 and 1132, weak or absent in the poly(Cbz-RhB), are assigned to Cbz in plane bending modes.

Aromatic Ring stretching and deformation (1300-1650 cm^{-1}) Vibration bands associated to aromatic C-N stretching expected from Rhodamines tertiary amines functions are usually present in the 1310-1360 cm^{-1} range [1]. The range is reasonably compatible with the band observed at 1308 cm^{-1}, which is observed at 1305 cm^{-1} in solid Rhodamine samples[2], and has alternatively been assigned to C-H deformation modes at the non-xanthenic ring [2]. Interestingly in the powder samples we rather observe a large band covering 1322-1361 cm^{-1}. Bands associated with C=C and C=N stretching due to ring deformation are observed in carbazoles at 1380 cm^{-1} and 1452 cm^{-1} [3,4], also observed in the poly(Cbz-RhB) at 1379 and 1454 cm^{-1} and in the monomeric dyad at 1380 and 1453 cm^{-1}. The first vibration appears at a similar frequency as symmetric deformations modes of pyrrole rings at 1384cm^{-1}[5], suggesting a similar deformation mode is observed here for the Cbz moieties. Analogies with other pyrrole ring deformations are also possible, such as antisymmetric ring deformation, observed at 1530

cm^{-1} for pyrroles[5] , at 1520-1540 cm^{-1} for solid carbazoles[3,4], which are also present at 1530 cm^{-1} in the monomeric dyads and at 1522 cm^{-1} for the polymeric layer.

Remaining bands are observed at 1493 cm^{-1} and 1465 cm^{-1}. The 1493 cm^{-1} band is consistent with 1490 cm^{-1} modes for carbazoles[3,4], and also observed in the dyad monomers at 1493 cm^{-1} . Due to the frequency region, characteristic of C=C stretching due to ring deformation, we broadly assign this band to deformation modes of the carbazoles moieties. The 1465 cm^{-1} band is present at the monomeric dyad at 1463 cm^{-1}. Similar bands are observed for Rhodamine solid samples, at 1463cm^{-1} [2]. This band is difficult to assign with certainty, as scissoring modes of aliphatic CH_2 moieties (present in the Rhodamines Xanthene ring substituents) typically appear in this frequency [1] but it could alternatively be assigned to ring deformation modes.

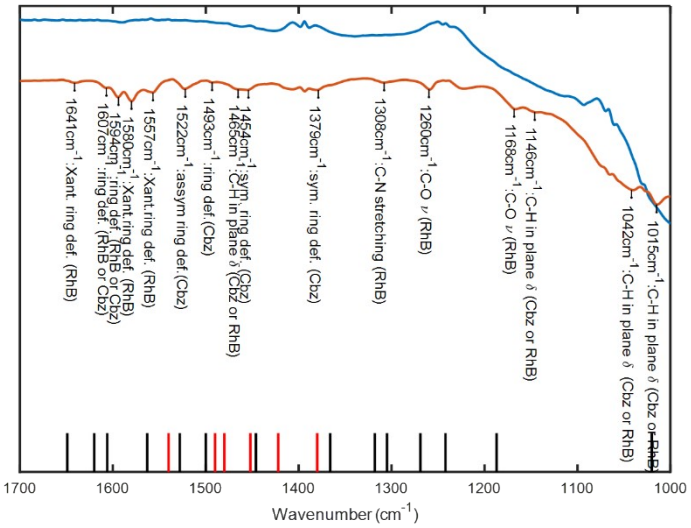

Figure S2.3 Focus on the 1000-1650 cm^{-1}region, indicating main observed vibrations, along with band assignment propositions. The bottom lines indicate Rhodamine and Carbazole vibration modes based on literature [2,4].

Finally, the band present at 1461 cm^{-1} on poly(Cbz-RhB), also observed at 1646 cm^{-1} on the monomeric dyad, is observed at solid Rhodamines at 1649 cm^{-1} [2]. It is assigned to modes associated with deformations of the xanthene ring, in analogy with anthracene modes observed at 1620-1640 cm^{-1}[6].

Out of plane C-H bending modes (Region 700-850 cm^{-1}) . The low wavenumber region, between 700 and 850 cm^{-1}, is usually dominated by C-H out of plane bending modes of aromatic rings, although some ring deformation modes can also appear in this region. Bands in this range are usually characteristic of the number of adjacent C-H bonds leading to characteristic vibration modes, enabling tentative assignments as indicated below.

As indicated in Fig. S2.4, the following bands can be observed: 700 cm^{-1}, 722 cm^{-1}, 728 cm^{-1}, 744 cm^{-1}, 761 cm^{-1}, 771 cm^{-1}, 791 cm^{-1} and 815 cm^{-1}.

Bands in the 720-735 cm^{-1} ring can be attributed to the 1,2 di-substituted aromatic rings [6]. In the dyad molecule, we observe a band on 726 cm^{-1} region, which becomes split in two in the poly(Cbz-RhB), leading to the bands at 722 and 728 cm^{-1}. The splitting of the band can be assigned to the presence of different environments, induced by steric hindrance due to polymerization of the monomer.

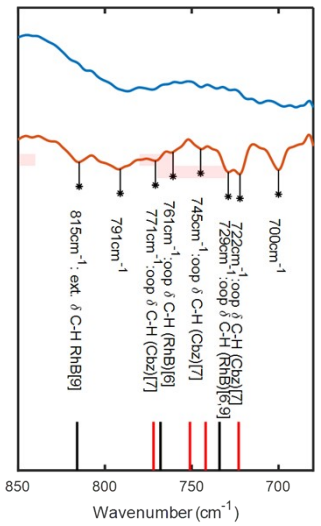

Figure S2.4. Focus on the 700-850 Cm^{-1} region, which contains modes commonly associated with out-of-plane C-H bending modes on aromatic compounds..

The band at 740-760 cm^{-1}, are also consistent with out of plane CH bending on 1,2 di-substituted aromatic compounds.[6] In the crystalline form, a strong band is present at 754 cm^{-1}, which gets largely perturbed in the poly(Cbz-RhB) layer. This observation suggests that the vibration is perturbed by polymerization, consistently with polymerization of Cbz moieties. Such modification is expected to generate 1,2,4 trisubstitued aromatic rings, whose characteristic δ_{OOP}(C-H) modes is expected in the 760 and 780 cm^{-1} [6]. Indeed, two bands are observable at 761 and 771 cm^{-1} on the polymerized region, further supporting

this assignment. A band at 815 cm^{-1} is observed at poly(Cbz-RhB), analogous to a mode observed at 822 cm^{-1} for the crystalline dyad. These modes are also consistent with 1,4-di substituted aromatic rings, and are observed at 816 for unsubstituted Rhodamines[2]. This supports the assignment of these modes to δ_{OOP}(C-H) on the non xanthetic ring of RhB.

Based on this reasoning, the following tentative band assignment is proposed. Evidence supporting polymerization reaction are shown in bold:

700	706	δ_{OOP} (C-H)	RhB/Cbz	Characteristic frequency region of OOP bending in aromatic molecules[1,6]. Present both on the dyad and polymerized region.
722	726	δ_{OOP} (C-H)	Cbz	Bands are observed at 720 and 723 cm^{-1} for solid carbazoles [4], for Rhodamines at 734 cm^{-1} [2] and at 726 for the crystalline dyad. Characteristic frequency region of 1,2- di-substituted aromatic rings.[6]
728	726	δ_{OOP} (C-H)	Cbz	
-	754	δ_{OOP} (C-H)	Cbz	Consistent with 1,2- di-substituted aromatic rings [1,6], observed for carbazoles at 740-742cm^{-1}[4],
761	-	δ_{OOP} (C-H)	Cbz	**Characteristic frequency of out of planes C-H bending on 1,2,4 trisubstituted rings[1,6]. In monomeric samples, an analogous band is observed at 756 cm^{-1} on carbazoles[4], and for the dyad at 754 cm^{-1} (characteristic of 1,2 di-substituted rings [6]), consistently with the polymerization reaction.**
771	-	δ_{OOP} (C-H)	Cbz	
815	822	δ_{OOP} (C-H)	RhB	Observed for Rhodamine samples at 816 cm^{-1} [2] and for the crystalline dyad at 822 cm^{-1}. Consistent with 1,2 disubstituted rings such as the non-xanthenic RhB [6].
1015	1011	δ_{IP} (C-H)	Cbz/RhB	Consistent with C-H in plane vibration modes in aromatic compounds, notably in 1,2 disubstituted rings [1,6]. Observed for rhodamines at 1020cm^{-1} and assigned to non-xanthenic C-H in plane bending modes [2] and at 1006, 1010 and 1022 cm^{-1}in solid Cbz samples. [4] Observed at 1011 cm^{-1} on the crystalline dyad.
1042	1047	δ_{IP} (C-H)	RhB	Consistent with C-H in plane vibration modes in aromatic compounds [1,6]. Observed at 1047 cm^{-1} in the crystalline dyad. Can alternatively be associated with 1020 cm^{-1} external ring modes, which are not modified by polymerization.
1076	1075	δ_{IP} (C-H)	Cbz	**Becomes very weak in the poly(Cbz-RhB).**
-	1132	δ_{IP} (C-H)	Cbz	**Region characteristic of C-H in plane bending on 1,2 disubstituted aromatic rings[6]. Observed at 1136^{-1} on solid Cbz [4]. Band only present in the monomeric dyad, and cannot be detected in the poly Cbz-RhB.**
1146	1156	$\delta_{IP}(C\text{-}H)^{ar}$	Cbz	Aromatic C-H in plane bending [1]. Band at 1136 cm^{-1} observed on solid Cbz samples[4].
1168	1180	ν(C-O)	RhB	Characteristic of C-O stretching frequencies on aliphatic esters (1163-1210 cm^{-1})[1] An analogous band is observed at 1180 cm^{-1} in the crystalline dyad.
1225	1246	ν(C-O)	RhB	Observed at 1242 on Rhodamines[2], associated to stretching modes of the external ring. Has alternatively been assigned to the C-O stretching mode of Rhodamines.
1260	1272	ν(C-N) or ν_{XR}(C-O)	Cbz/RhB	Band at 1270 cm^{-1} observed on solid Cbz[4] and alternatively can be assigned to C-O streching of the xanthenic ring, as it has been observed at 1269 cm^{-1} on solid Rhodamines [2]
1308	1320-1358	ν(C-N)	RhB	Region characteristic of C-N stretching in terciary aromatic amines [1]. Observed at 1305cm^{-1} in solid Rhodamine 6G [2]. Although compatible with C-N stretching, this band has also been assigned in literature to C-H deformation[2]
1379	1380	ν_s (C=N/C=C) ring def.	Cbz	Observed for carbazoles and for the monomeric dyad at 1380 cm^{-1} [4] Analogous to pyrrole mode at 1384 cm^{-1} [5]
1454	1453	ν (C=N)	Cbz	Observed for carbazoles at 1452cm^{-1}[4]
1465	1463	$\delta_{scissoring}$ (CH_2)	RhB	Characteristic frequency for C-H scissoring bending modes in aliphatic CH_2 groups [1]. Can alternatively be assigned to C=C stretching. [1,6]. Observed for solid Rhodamine solid samples at 1463 cm^{-1}. [2]
1493	1493	$\nu(C{=}C)^{ar}$ ring def.	Cbz	Characteristic C=C stretching in aromatic moieties [1]. Observed for Carbazoles at 1490 cm^{-1} [3,4]

1522	1530	ν_{as}(C=N/C=C) ring. Def.	Cbz	Observed for carbazoles in the 1520-1540 cm^{-1} range [3,4], Analogous to pyrrole assymetric deformation mode at 1530 cm^{-1} [5]
1557	1554	ν(C=C) ^{ar} Xanthene ring def	RhB	Observed at Rhodamines at 1563 cm^{-1} [2]. Attributed to deformation modes of the xanthene ring[2], analogous to similar modes present in anthracene at 1550 cm^{-1} [6]
1580	1587	ν(C=C)^{ar}	RhB/Cbz	Aromatic C=C stretching group frequencies[1,6] bands in this position are usually observed for six-membered rings on which conjugation is extended [6].
1594	1587	ν(C=C)^{ar}	RhB	Aromatic C=C stretching group frequency [1,6]
1607	1587	ν(C=C)^{ar}	Cbz/RhB	1606 cm^{-1} observed at Rhodamine 6G [2] can alternatively also be associated with Cbz band observed at 1620 cm^{-1} [4]
1641	1646	ν(C=C) ^{ar} Xanthene Ring def	RhB	Observed for Rhodamines at 1649 cm^{-1}[2] Analogous to anthracene mode at 1620-1640 cm^{-1}[6]
1729	1720	ν (C=O)	RhB	Group frequency on the 1700-1800 region [1]. Band observed at 1718 cm^{-1} on solid Rhodamine 6G[2] and at 1720 cm^{-1} on the crystalline dyad.
1747	1720	ν (C=O)	RhB	

References

[1] Hermann, C.K.F.; Morrill, C.; Shriner R.L.; Fuson R.C. "Ch. 2 Infrared Spectroscopy " in "The systematic identification of organic compounds" Wiley 8th Edition.

[2] Lajoube M. and Henry, M. "Fourier transform raman and infrared and surface enhanced Raman spectra for rhodamine 6G." Spectrochimica Acta A 47, 9/10, 1459-1466 (1991).

[3] Jana S, Trivedi MK, Branton A, Trivedi D, Nayak G, et al. (2015) Physical and Structural Characterization of Biofield Energy Treated Carbazole. Pharm Anal Acta 6: 435. doi:10.4172/21532435.1000435

[4] Vibrational assignment of carbazole from Infrared Raman and Fluorescence Spectra J. Chem Phys 49 3344 (1968)

[5] Katritzky A.R., "The infrared spectra of heteroaromatic compounds" Q. Rev. Chem. Soc., 13, 353-373 (1959).

[6] Socrates G. "Infrared and Raman Characteristic Group Frequencies: Tables and Charts" 3rd ed. Wiley

Section S3) Fluorescence images of photografted patterns

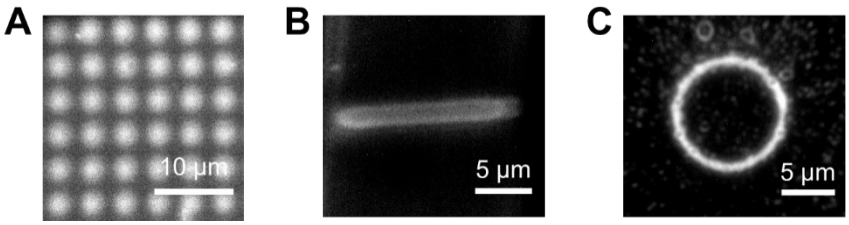

Figure S3.1 Fluorescence image of different surface patterns obtained by photopolymerizing Cbz-RhB dyad into poly carbazole rhodamine layers. (A) Grid pattern, used to collect the IR data discussed in Sect. S2. (B) Wire pattern connecting two gold electrodes (AFM image reported on Fig. 5B).(C) Circle pattern, as reported in Fig.4D. For all images λ_{exc}*= 560 nm, with exposition times on the 100 ms range.*

The stability of the fluorescence emission of polymerized layers is evaluated by monitoring the intensity of the emission of the grid pattern (Fig.S3.1 A) over time, under illumination density of 50 W/cm^2 ($^{\lambda_{exc}} =$ 474 nm, 40MHz).

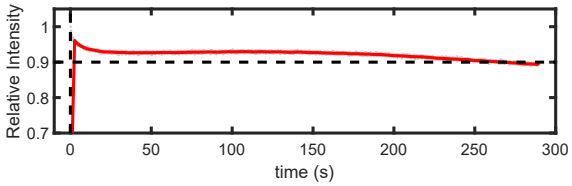

Figure S3.2 Monitoring of the fluorescence emission of the pattern shown in Fig.S3.1A.

Section S4) Routine for trajectory preparation in direct laser writing

Trajectories for direct laser writing experiments were calculated based on control points provided by the user with the routine described in this section. The original control points are first interpolated with 3rd order spline functions. An iterative procedure is then put in place to homogenize the distance between control points on which each trajectory is reinterpolated, over a number of new control points which is proportional to the distance between the original control points. After a few (typ.3-4) iterations, the distance between neighbouring points converges towards a fixed value, ensuring that a homogeneous velocity during the whole operation.

Section S5) Influence of speed on patterns thickness and height

In this section, we report the influence of the piezo displacement speed on the properties of the resulting lines. This data is obtained by extracting a large number (N=30) of profiles from the AFM images shown in Figs.4B and 4C of the main text, and fitting each profile with a gaussian function

$$F(x) = He^{-\left(\frac{(x-\mu)}{2\sigma}\right)^2}$$

The amplitude H of the gaussian is used as the height, while the dispersion σ is used to evaluate the full width at half maximum FWHM = 2σ $(\ln(2))^{0.5}$. This procedure leads to the data indicated in the figure S4

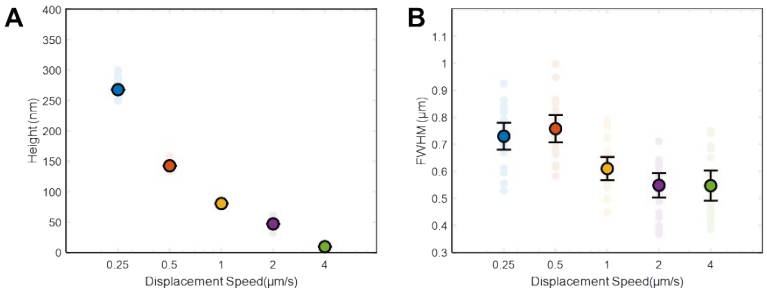

Figure S5.1 Influence of the piezo displacement speed on the lines (A) Height and (B) width. This analysis is performed on the data shown in fig 4 of the main text.